Table 2 Summarized results of case 1 and case 2

Case	$k(\Psi^a)$	$\|K\|_{\text{fro}}$	$\|KC_r\|_{\text{fro}}$	$\|\Psi^T(KC_r)\|_{\text{fro}}$
1	263.5680	113.1525	60.7262	3.0335
2	2801.7103	113.0615	47.0881	2.6789

As a result, the norm of the observation spillover term $\|KC_r\|_{\text{fro}}$ is 60.7262. In this case, spillover instability occurs, which can be easily verified from the eigenvalues of the composite system in Eq. (6) as described in Table 1 (case 1). The underlined eigenvalues in case 1, which are shifted by spillover, makes the entire feedback control system unstable.

Next, in the second case (case 2), the achievable parameter matrix H^a is obtained as follows:

$$H^a = \begin{bmatrix} -10.7076 & -20.5166 & -11.0363 & 13.5645 \\ 7.9923 & 14.7979 & 9.9422 & -12.0749 \\ -2.0429 & -2.8253 & -5.7019 & 6.7023 \\ -2.6599 & -6.3837 & 1.5093 & -1.4936 \end{bmatrix}$$

In addition, the condition number of the achievable modal matrix $k(\Psi^a)$ is 2081.7103. Then, the observer gain matrix K and its Frobenious norm are calculated as follows:

$$K = \begin{bmatrix} -11.5548 & -13.9220 & 45.3413 & -59.0716 \\ -49.3056 & 50.2492 & -37.7653 & 21.2715 \\ 2.5023 & -0.5594 & -2.2824 & 3.8838 \\ 3.7553 & -4.1166 & 3.4873 & -2.3422 \end{bmatrix}$$

$$\|K\|_{\text{fro}} = 113.0615$$

As a result, the norm of the observation spillover term $\|KC_r\|_{\text{fro}}$ is 47.0881. In this case, the stable entire feedback control system is obtained by suppressing the observation spillover, which can be seen from the eigenvalues of the composite system in Table 1 (case 2).

In simulations, two cases of observer design are compared in almost the same norm condition of K as seen in Table 2. In case 1, we achieve a minimum condition number of Ψ^a for the preassigned eigenvalues, but it can not avoid spillover instability. On the other hand, in case 2, the condition number $k(\Psi^a)$ increases compared with case 1 because some part of the design freedom for eigenvectors is used to design the parameter vectors to satisfy condition 1. However, we can reduce the norm of the observation spillover term KC_r, and spillover instability in case 1 is recovered. Consequently, the observer design in case 2 has shown to be more effective and successful in spillover suppression than that of case 1 in which the spillover suppression is dealt with simply as a robust stability problem.

VI. Conclusions

This Note presents a new spillover suppression method using eigenstructure assignment, which can prevent possible instability in the active control of large flexible structures caused by the neglected dynamics of the higher modes of vibration by reducing their detrimental effect of spillover. In simulations, by the comparison of two cases of observer design, the proposed method has been proven to be successful in the spillover suppression of large flexible structures.

Acknowledgments

This work was supported in part by Grant 2001-1-30200-004-2 from the Basic Research Program of the Korea Science and Engineering Foundation. The first author was supported by the Brain Korea 21 Program.

References

[1]Hyland, D. C., Junkins, J. L., and Longman, R. W., "Active Control Technology for Large Space Structures," *Journal of Guidance, Control, and Dynamics*, Vol. 16, No. 5, 1993, pp. 801–821.

[2]Balas, M. J., "Active Control of Flexible Systems," *Journal of Optimization Theory and Applications*, Vol. 25, No. 3, 1978, pp. 415–436.

[3]Balas, M. J., "Feedback Control of Flexible Systems," *IEEE Transactions on Automatic Control*, Vol. AC-23, No. 4, 1978, pp. 673–679.

[4]Meirovitch, L., and Baruh, H., "On the Problem of Observation Spillover in Self-Adjoint Distributed-Parameter Systems," *Journal of Optimization Theory and Applications*, Vol. 39, No. 2, 1983, pp. 269–291.

[5]Zhang, Q., Slater, G. L., and Allemang, R. J., "Suppression of Undesired Inputs of Linear Systems by Eigenspace Assignment," *Journal of Guidance, Control, and Dynamics*, Vol. 13, No. 2, 1990, pp. 330–336.

[6]Choi, J. W., Lee, J. G., Kim, Y., and Kang, T., "Design of an Effective Controller via Disturbance Accommodating Left Eigenstructure Assignment," *Journal of Guidance, Control, and Dynamics*, Vol. 18, No. 2, 1995, pp. 347–354.

[7]Junkins, J. L., and Kim, Y., *Introduction to Dynamics and Control of Flexible Structures*, AIAA Education Series, AIAA, Washington, DC, 1993, pp. 35–49.

[8]Chen, C. T., *Linear System Theory and Design*, Holt, Rinehart, and Winston, New York, 1979, pp. 324–378.

[9]Klein, G., and Moore, B. C., "Eigenvalue-Generalized Eigenvector Assignment with State Feedback," *IEEE Transactions on Automatic Control*, Vol. 22, No. 1, 1977, pp. 140, 141.

[10]Andry, A. N., Jr., Shapiro, E. Y., and Chung, J. C., "Eigenstructure Assignment for Linear Systems," *IEEE Transactions on Aerospace and Electronic Systems*, Vol. AES-19, No. 5, 1983, pp. 711–729.

Solar Sail Hybrid Trajectory Optimization for Non-Keplerian Orbit Transfers

Gareth W. Hughes* and Colin R. McInnes†
University of Glasgow, Glasgow, Scotland G12 8QQ, United Kingdom

Introduction

SOLAR sails have long been seen as an attractive concept for low-thrust propulsion. They transcend reliance on reaction mass and have the ability to provide a small, but continuous, acceleration. Because propellant mass is not an issue, high-performance sails can enable new exotic non-Keplerian orbits (NKOs)[1] that are not feasible for conventional chemical or electric propulsion. A constant out-of-plane sail force is utilized to raise the spacecraft's orbit high above the ecliptic plane in two- or three-body systems. Potential benefits to the science community are large. Circular, displaced orbits can be used to provide continuous observation of the solar poles or to provide a unique vantage point for infrared astronomy. (There is much less resolution-limiting dust out of the ecliptic plane enabling smaller telescope mirror dimensions for equivalent performance.) Very-high-performance sails can even levitate, in equilibrium, at any point in space.

Three parameters of the NKO determine what sail acceleration and orientation is required: the vertical displacement z above the ecliptic plane in the direction of the ecliptic normal, the horizontal distance ρ from the sun in the ecliptic plane, and the orbit period T, which is usually taken to be one year so that the sail orbits synchronously with the Earth. The sail lightness number β is defined as the ratio of the sail characteristic acceleration [solar radiation pressure induced acceleration at 1 astronomical unit (AU)] to the solar gravitational acceleration at 1 AU. Because both have an inverse square form, the sail lightness number is a dimensionless constant.

Received 9 July 2001; revision received 8 January 2002; accepted for publication 9 January 2002.

*Postgraduate Student, Department of Aerospace Engineering; ghughes@aero.gla.ac.uk.

†Professor, Department of Aerospace Engineering; colinmc@aero.gla.ac.uk.

The thrust-vector orientation is specified by two angles, the cone angle α, that is, the angle between the sail normal (the thrust vector, for an ideal sail) and the sun line $\alpha \in [-\pi/2, \pi/2]$, and the clock angle δ, that is, the angle between the projection of the sail normal and some reference direction onto a plane normal to the sun line $\delta \in [0, \pi]$ (Ref. 1). For a circular displaced NKO, the clock angle is zero because only an out-of-plane force is necessary, and β and α are determined by the following equations[1]:

$$\tan\alpha = \frac{(z/\rho)(\omega/\tilde{\omega})^2}{(z/\rho)^2 + [1 - (\omega/\tilde{\omega})^2]} \tag{1}$$

$$\beta = \left[1 + \left(\frac{z}{\rho}\right)^2\right]^{\frac{1}{2}} \frac{\{(z/\rho)^2 + [1 - (\omega/\tilde{\omega})^2]^2\}^{\frac{3}{2}}}{\{(z/\rho)^2 + [1 - (\omega/\tilde{\omega})^2]\}^2} \tag{2}$$

where ω is the orbital angular velocity $(2\pi/T)$ and $\tilde{\omega} = \sqrt{(\mu/r^3)}$, where the gravitational parameter $\mu = GM_{\text{sun}} = 1$ in canonical units and $r = \sqrt{(\rho^2 + z^2)}$ is the radial distance from the sun (constant for a circular NKO).

Although the conditions for families of NKOs have been known,[1] transfers to such orbits have not yet been investigated. This can be achieved by using the solar sail to perform a minimum time spiral to the NKO from the Earth. A direct optimization method was used to optimize the transfers, which hybridized a genetic algorithm (GA) method with a sequential quadratic programming (SQP) algorithm. The equations of motion were integrated in singularity free modified equinoctial orbital elements for efficiency and accuracy.[2]

Hybrid Optimization Method

Direct trajectory optimization was used to select a discrete sequence of control angles that null the endpoint errors between the spacecraft final state vector and the target state vector while minimizing the total transfer time. The trajectory was divided into equal duration segments, each with a different fixed sail cone and clock angle increment, providing an approximation to the true minimum-time transfer. True optimal transfers can be achieved by a hypothetical increase of the number of segments to infinity, giving a continuous steering time history, effectively the same as using the calculus of variations method of optimal control theory.[3] However, the calculus of variations is highly sensitive to initial costate estimates. Tracking a fixed sail orientation would be easier to implement in practice than some complex time-varying profile, and it might be possible to have passive stability of the sail attitude relative to the sun line. An efficient method of constrained optimization is the SQP algorithm, which employs a quasi-Newton method to directly solve the Karush–Kuhn–Tucker conditions of optimality. The main pitfall with this kind of nonlinear programming is that, although it is more robust than the calculus of variations, it is also a local optimizer searching from an initial point and evolves in the direction of steepest search-space gradient. Therefore, an understanding of the problem is required. However, transfers to NKOs are totally new, and NKO transfer control angles are not immediately obvious; thus, the global optimization capability of a GA was used to provide an initial guess for the SQP algorithm.

GAs are based on the Darwinian concept of natural selection and survival of the fittest.[4] GAs differ from conventional optimization algorithms in that they search from a population of points, and hence, a global picture of the search space can be visualized, but they have poor convergence properties. Constraints are problematic to incorporate in a single-valued GA fitness function and so the transfer time was kept fixed. (A reasonable guess was required.) The fitness function was formulated in terms of the spherical polar endpoint constraints. A number of genetic operators are executed as evolution proceeds through reproduction. Tournament selection compares two individuals at random and lets the one with the highest fitness go on to reproduce. This process is repeated until the whole population is covered. Single-point crossover facilitates information exchange between the selected parents and randomly interchanges sections of the parent's genomes. Mutation helps maintain genetic diversity in the population by randomly flipping a bit in the chromosome.[5] One special operator used was elitism, which copies the fittest individual from one generation to the next to prevent it inadvertently being lost. This was consistent with previous authors who used the GA alone to reach inner planets and small bodies, but not to reach displaced NKOs.[5,6] The population size was 2000, maximum number of generations was 300, and the crossover probability of 0.6 and mutation probability of 0.0015 were the same as those used by Rauwolf and Friedlander.[5]

Different hybrid approaches to low-thrust optimization have also been adopted by previous authors using the calculus of variations.[7] For this hybridization technique, the boundary conditions and lightness number were calculated from the desired NKO dimensions. Then an estimate of the transfer time was supplied to the fixed-time GA. The GA was allowed to evolve to find the minimum endpoint errors for that transfer time. The resulting cone and clock angles were, thus, in the region of the search space where the global optimum resided. These control angles were then passed to the SQP algorithm for fine tuning, to minimize the transfer time while enforcing the endpoint equality constraints. If the solution produced a transfer time that was thought to be a local optimum (even though there were no previous studies to refer to), then the hybrid optimizer was started again with an accordingly adjusted initial guess of the transfer time for the GA. The initial guess produced by the GA for one transfer was occasionally used for other similar transfers with the SQP alone because the optimum region of the search space had been identified.

NKO Transfers

A transfer to an NKO entails an optimization that only enforces five constraints because the final azimuth angle is free. This was an easier problem for the hybrid optimizer to solve than the constrained problem of the next section. Table 1 shows optimal transfer times to different dimension NKOs, with their corresponding lightness numbers, for differing numbers of control segments. It can be seen that as the number of segments is reduced there is a relatively small penalty in transfer time for the NKOs that are more easily reached. The transfers to a 0.3×0.7 AU, one year NKO are shown in Fig. 1 for 3, 4, 5, and 10 segments. Table 2 shows dependency of β on z and ρ.

For telemetry purposes, it would be desirable to have future science spacecraft deployed on NKO that are synchronous with the Earth and at a point directly above the sun–Earth line. Because the Earth's orbit is approximately circular, this is feasible. The trajectory analysis was extended to include Earth ephemerides, calculated using an analytical approximation. Figure 2 shows the trajectory for launch on 29 July 2001, and Fig. 3 shows the cone and clock angle time histories for four control segments. In the initial and final

Table 1 Optimal transfers to displaced NKOs

Number of control segments	Transfer time (days)		
	$\beta = 0.43$	$\beta = 0.88$	$\beta = 0.97$
3	173.02	222.88	255.84
4	161.43	210.88	238.33
5	159.86	207.48	230.63
10	158.99	202.71	224.08

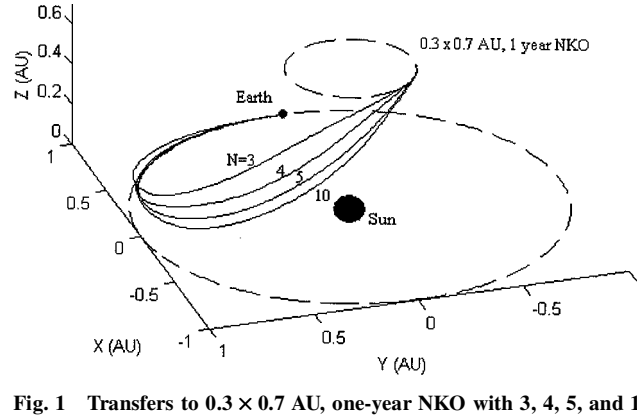

Fig. 1 Transfers to 0.3×0.7 AU, one-year NKO with 3, 4, 5, and 10 segments.

Table 2 Sail lightness β as dependent on vertical displacement above ecliptic pole, z, and horizontal displacement from ecliptic pole, ρ

z, AU	ρ, AU	β
0.2	0.9	0.43
0.5	0.5	0.88
0.7	0.3	0.97

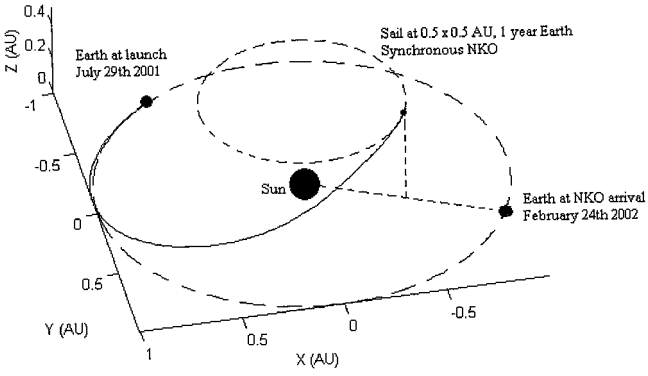

Fig. 2 Four-segment transfer to Earth synchronous 0.5 × 0.5 AU, one-year NKO launched 29 July 2001.

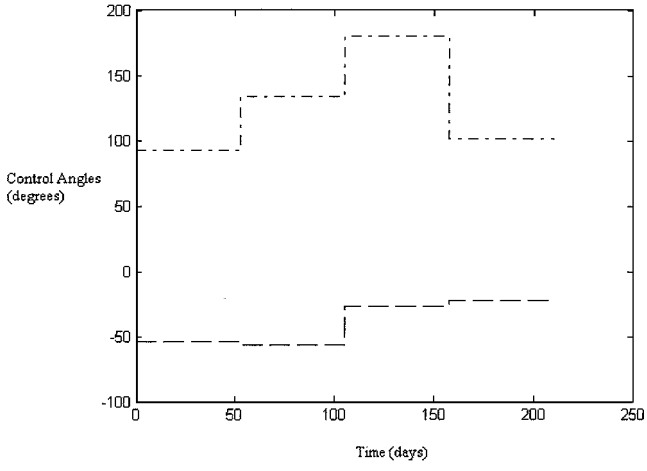

Fig. 3 Control angle history for transfer to Earth synchronous 0.5 × 0.5 AU, one-year NKO: – – –, cone angle; and –·–·–, clock angle.

stages of the transfer, the thrust was directed mostly in the opposite direction to the velocity vector; for the intermediate stage, the thrust is an almost entirely out-of-plane.

Conclusions

A trajectory optimization tool has been developed which hybridized a GA with SQP. When applied to the difficult problem of preliminary mission planning for high-performance solar sail transfers to displaced NKOs, it appeared to identify near-optimal trajectories with relative ease. The transfer time penalties (estimated from transfer time convergence as the number of segments was increased) appear acceptable even for a small number of segments (four or five). A small number of segments reduced the computational burden imposed by using a GA and would simplify attitude control in practice.

Acknowledgment

The genetic algorithm was developed by D. L. Carroll of the University of Illinois.

References

[1]McInnes, C. R., *Solar Sailing: Technology, Dynamics and Mission Applications*, Springer-Praxis Series in Space Science and Technology, Springer-Verlag, Berlin, 1999, pp. 171–228.

[2]Walker, M. J. H., Ireland, B., and Owens, J., "A Set of Modified Equinoctial Orbit Elements," *Celestial Mechanics*, Vol. 36, 1985, pp. 409–419.

[3]Bryson, A. E., Jr., and Ho, Y. C., *Applied Optimal Control*, Hemisphere, New York, 1975, pp. 42–69.

[4]Goldberg, D. E., *Genetic Algorithms in Search, Optimization, and Machine Learning*, Addison Wesley Longman, Reading, MA, 1989.

[5]Rauwolf, G. A., and Friedlander, A., "Near-Optimal Solar Sail Trajectories Generated by a Genetic Algorithm," American Astronautical Society/AIAA Astrodynamics Specialists Conf., AAS Paper 99-332, Aug. 1999.

[6]Fowler, W. T., Crain, T., and Eisenreich, J., "The Influence of Coordinate System Selection on Genetic Algorithm Optimization of Low-Thrust Spacecraft Trajectories," American Astronautical Society/AIAA Spaceflight Mechanics Meeting, AAS Paper 99-130, Feb. 1999.

[7]Coverstone-Carroll, V., Hartmann, J. W., and Mason, W. J., "Optimal Multi-Objective Low-Thrust Spacecraft Trajectories," *Computer Methods in Applied Mechanics and Engineering*, Vol. 186, 2000, pp. 387–402.

Optimal Earth-Capture Trajectories Using Electric Propulsion

C. A. Kluever*
University of Missouri–Columbia, Columbia, Missouri 65211

Introduction

With the success of Deep Space 1, electric propulsion (EP) has become a viable propulsion option for performing interplanetary space missions.[1] One potential interplanetary application of EP is for the Earth-return leg of a sample return mission.[2] In this scenario, EP would eventually perform the capture maneuver from hyperbolic approach to a closed Earth orbit. It appears that research involving optimal EP capture trajectories, especially transfers involving hundreds of orbital revolutions, is somewhat limited. Battin[3] presented a feasible scheme for performing capture trajectories into a low lunar orbit with a variable low-thrust engine. Recently, Vadali et al.[2] demonstrated a Lyapunov feedback control law for performing a low-thrust capture into a high-altitude Earth elliptical orbit. In this Note, a new approach for computing optimal Earth-capture trajectories is presented. This approach joins numerically integrated trajectories with curve fits of universal low-thrust solutions to represent efficiently and accurately the complete capture phase. Numerical results are presented for minimum-propellant trajectories.

System Model

The Earth-capture trajectory is governed by the following dynamic equations:

$$\dot{\boldsymbol{r}} = \boldsymbol{v} \tag{1}$$

$$\dot{\boldsymbol{v}} = -\frac{\mu \boldsymbol{r}}{r^3} + \boldsymbol{a}_P + \boldsymbol{a}_T \tag{2}$$

$$\dot{m} = \frac{-2\eta P}{(g I_{\mathrm{sp}})^2} \tag{3}$$

where $\boldsymbol{r}$ and $\boldsymbol{v}$ are the position and velocity vectors of the spacecraft in an Earth-centered inertial (ECI) Cartesian frame, μ is the Earth gravitational constant, $\boldsymbol{a}_P$ is an acceleration vector due to perturbations, and $\boldsymbol{a}_T$ is the thrust acceleration vector. Equation (3) defines the mass loss due to the low-thrust engine where m is spacecraft

Received 21 August 2001; revision received 17 January 2002; accepted for publication 17 January 2002.

*Associate Professor, Mechanical and Aerospace Engineering Department. Associate Fellow AIAA.